Available online at www.sciencedirect.com

ScienceDirect

Energy Procedia 1 (2009) 3129–3133

Energy Procedia

www.elsevier.com/locate/procedia

GHGT-9

# Viscosity and Electrical Conductivity of Aqueous NaCl Solutions with Dissolved $CO_2$.

Marc Fleury, Hervé Deschamps

*IFP, Petrophysics Dpt, 1, avenue de Bois-Préau, Rueil-Malmaison, 92852, France*

**Abstract**

With the perspective of long term $CO_2$ storage, thermodynamic data are necessary for the simulations of $CO_2$ injection in aquifers of depleted oil reservoirs. We focus here on the determination of the resistivity and viscosity of aqueous NaCl solutions with dissolved $CO_2$. It is well known that dissolved $CO_2$ increases slightly the water density. Recently, Bando et al. (2004) measured the viscosity of $CO_2$ saturated brines and found an increase of viscosity with increasing amount of dissolved $CO_2$. For resistivity, no data is available to our knowledge.

We evaluated the effect of dissolved $CO_2$ simultaneously on the resistivity and viscosity of three NaCl solutions covering the range of salinity usually encountered in potential $CO_2$ storage geological formations. At a constant temperature of 35°C, we show that the variation of resistivity and viscosity are proportional to the amount of dissolved $CO_2$. For viscosity, our data are in agreement with previous observations. The observed variations are small, at maximum of the order of 10%. The increase of viscosity is well correlated with the variation of conductivity because ions are moving in a more viscous solvent and therefore conductivity decreases. For the temperature dependence, we used the Arps model to describe the measured variation of conductivity as a function of temperature. We propose a simple model to take into account the small modifications of conductivity and viscosity as a function of the dissolved $CO_2$ fraction and temperature. Finally, we examine two potential impacts of these findings.



*Keywords:* CO2, viscosity, conductivity, resistivity ;

## 1. Introduction

Dissolved acid gases have specific physical properties due to their interactions with the solvent that are difficult to predict. For $CO_2$, a peculiar behavior is the increase of viscosity when dissolved into water [1]. Even though only a small mole fraction of $CO_2$ can be dissolved at elevated pressure (i.e. about 2%), the viscosity can increase by 10% whereas the density only increases by 1%. Since viscosity, ionic conductivity (and diffusion) are closely linked, such behavior motivated us to study simultaneously the conductivity and viscosity of aqueous NaCl solutions

doi:10.1016/j.egypro.2009.02.094

containing dissolved $CO_2$. For conductivity, we expect to find a decrease of conductivity but the complex ions hydrodynamical interactions [2] at high salt concentrations is rather difficult to predict. We first present the simultaneous measurements of the variation of conductivity and viscosity for three NaCl brine of salinity 20, 80 and 160 g/L, (respectively 0.342, 1.369 and 2.738 mol/L), representative of the range of salinity encountered in geological formation. Then, we discuss some practical impact in terms of resistivity monitoring and convective motions.

## 2. Experimental technique

The variations of viscosity $\eta$ and conductivity $\kappa$ were deduced from the measurements of the variations of pressure drop $dP$ when flowing $CO_2$ saturated solutions across a porous medium, and the measurements of the variations of resistance $R$ of this porous media (Figure 1). From the Darcy's and Ohm's laws, we have:

$$\eta = \frac{SK}{LQ} dP \qquad \kappa = \frac{1}{f_{cell} R} \tag{1}$$

where $L$ and $S$ are respectively the length and surface area of the porous medium, $Q$ is the flow rate, $K$ is the permeability, $f_{cell}$ is a geometric cell factor [m]. If all these factors are kept constant, the variations of $dP$ and $R$ can be used to characterize the variations of viscosity and conductivity. The resistance $R$ depends essentially on the porosity, while permeability depends essentially on the connections between pores.

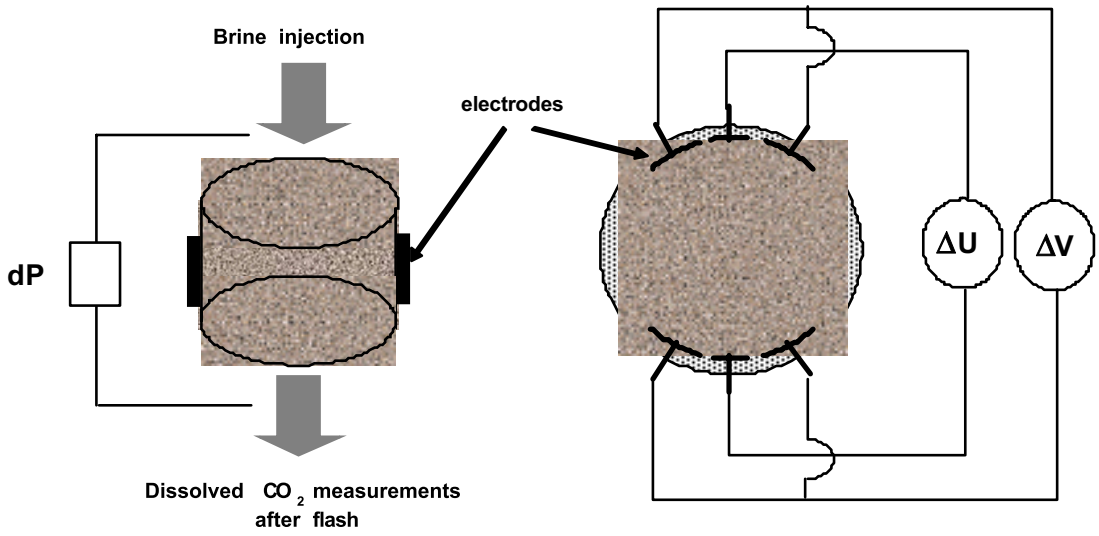


Figure 1: Schematic of the experimental set-up. A porous ceramic was used to measure the variation of pressure drop and resistance when flooding with NaCl solutions with and without dissolved CO2.

The resistance of the porous media was measured using a set of six electrodes located radially around the sample (Figure 1); two pairs of large electrodes are used to inject the current (500 mV, 1 kHz) and the small electrode pair is used to measure the voltage drop. The electrodes are molded in a Viton sleeve which is also used to apply a confining pressure on the sample. The electrodes are connected to an impedance meter (Agilent 4263) and the resistance is determined from the real part of the measured complex impedance. Therefore, we avoid contact resistance, and hydraulic flow and electric current injection are separated and do not interact each other.

The aqueous NaCl solutions were prepared using de-ionized water. To dissolve a given amount of $CO_2$, the solutions were placed in a high pressure Hastelloy container filled at mid-level. Then, $CO_2$ was injected at the top and the pressure imposed at a value varying from 1.0 up to 8.0 MPa in order to obtain variable amounts of dissolved $CO_2$ into the brine. To insure thermodynamic equilibrium, the container was agitated several times. Then the excess $CO_2$ is removed, the pressure increased up to 8.5 MPa (for all experiments) and the solutions injected through the

porous media. To obtain a sealing between the sample and the sleeve, the confining pressure was fixed at 13.5 MPa for all experiments, the temperature of the flooding cell fixed at 35 °C (in a temperature regulated oven) except for the measurements performed at variable temperature described later. The exact amount of dissolved $CO_2$ was measured after the resistance and pressure drop measurements. This was performed for each experiment on 5 liquid samples using volumetric brine and gas measurements after a flash and separation at ambient pressure and temperature. The conversion from gas volume to mole fraction $x_{CO2}$ takes into account the measured temperature.

The procedure for both resistance and pressure drop measurements is as follows: the brine without $CO_2$ is first injected at a constant low flow rate of 1 $cm^3 \cdot h^{-1}$ through the porous ceramic to determine a reference resistance and pressure drop. Then the brine with dissolved $CO_2$ is injected and the variation of resistance and pressure drop recorded. Finally, the initial brine is injected again to verify that no modification of the porous ceramic occurred during the $CO_2$ flooding. This procedure is repeated for every experiment when varying the dissolved $CO_2$ mole fraction. Due to the appropriate choice of the porous ceramic both in terms of permeability and porosity, the variations of resistance and pressure drop are easily measured using standard equipment (up to 20 Ω for $R$ and up to $7x10^4$ Pa for $dP$). The source of uncertainties is mostly due to the baseline fluctuations, a result of the slight modifications of the porous media. The measurements at variable temperatures were performed using a continuous increase of the oven temperature while keeping the pore and confining pressures constant.

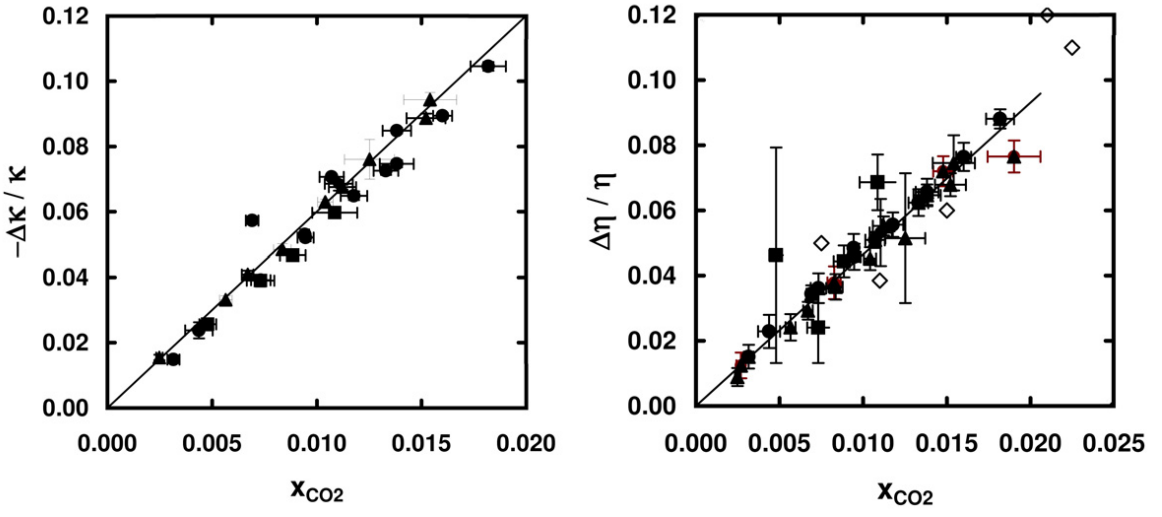


Figure 2: Relative variation of conductivity κ and viscosity η at 35 °C for three salinities; • 20 g/L ; ▲ 80 g/L ; ■ 160 g/L. .

## 3. Results

We found a linear relationship between the relative variation of resistance and the measured mole fraction $x_{CO2}$ of dissolved $CO_2$ ( regression coefficient 0.99, Figure 2):

$$\frac{\Delta\kappa}{\kappa} = -6.0 \; x_{CO2} \tag{2}$$

Note that despite the formation of additional ions due to the dissociation of $CO_2$ in water ( $H^+, HCO_3^-$ ), conductivity decreases. However, these ions represent a very small fraction relative to NaCl. Indeed, assuming a pH of 3, the $H^+$ concentration will be about $10^{-3}$ mol/L (by definition), while the NaCl concentration will be more than hundred times larger (0.342 mol/L for 20g/L). Similarly for viscosity, the relative variation of the differential pressure is also related linearly to the amount of dissolved $CO_2$ (regression coefficient 0.97, Figure 2):

$$\frac{\Delta\eta}{\eta} = 4.65\ x_{CO2} \tag{3}$$

For comparison we plotted a few data points from the work of Bando et al. [1]. They are in agreement with our observations. Note that there is no salinity dependence. However, the amount of dissolved $CO_2$ is smaller for the highest salinity (0.01 for 160 g/L instead of 0.025 for 20g/l), as expected from dissolution studies.

For the temperature dependence, we tested the formulation currently used for resistivity (Arps empirical formulae [3]). For the 20 g/L NaCl solution, the evolution the conductivity with and without dissolved $CO_2$ can be fitted with the following relationship (Figure 3):

$$\kappa_S(T) = \kappa_S(T_0)\ \frac{T + 19.5}{T_0 + 19.5} \qquad 35\ °C < T < 100\ °C \tag{4}$$

The value 19.5 in the above equation was first adjusted to the data without dissolved $CO_2$. Using the same value with dissolved $CO_2$, the fit is slightly less accurate (largest deviation of 1.9 % instead of 0.4%). For viscosity, the same law can be applied because the variations of differential pressure were linearly related to the variation of resistance when increasing the temperature (not shown).

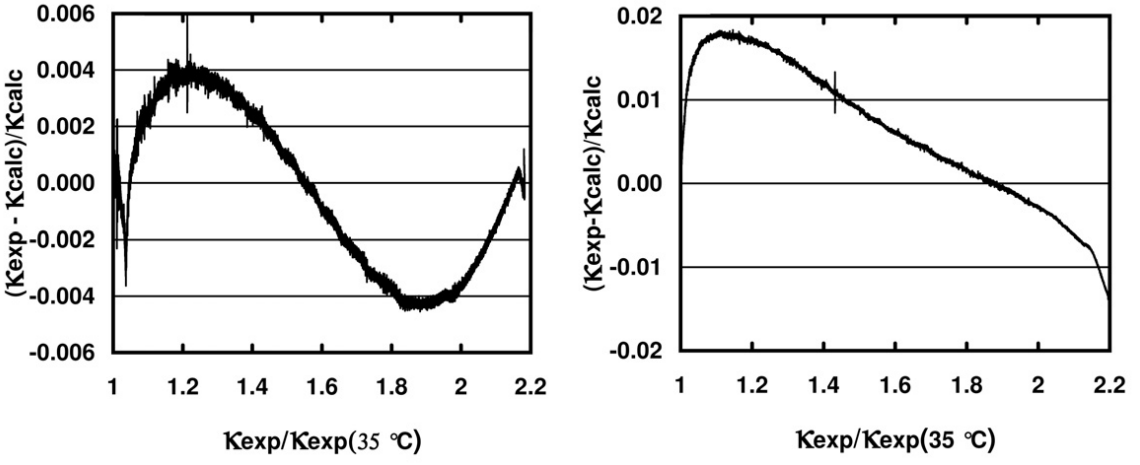


Figure 3: Deviation of measured conductivity $\kappa_{exp}$ from calculated conductivity $\kappa_{calc}$ using the Arps formulation, without dissolved $CO_2$ (left) and with dissolved $CO_2$ (right, $x_{CO2}$=0.011). $C_{NaCl}$ = 20 g/L, pressure 8.5 MPa. The temperature was varied continuously between 35 and 100 °C.

Finally, combining the temperature and dissolved $CO_2$ dependences, we can propose the following relationships describing the effect of dissolved $CO_2$ on electrical conductivity $\kappa$ and viscosity $\eta$:

$$\kappa_S(x_{CO2}, T) = \kappa_S(0, T_0)\ (1 - 6.0 x_{CO2}) \left(\frac{T + 19.5}{T_0 + 19.5}\right) \tag{5}$$

$$\eta_S(x_{CO2}, T) = \eta_S(0, T_0)\ (1 + 4.65\, x_{CO2}) \left(\frac{T_0 + 19.5}{T + 19.5}\right) \tag{6}$$

## 4. Practical impact

We discuss here two applications in which the decrease of conductivity and the increase of viscosity may have an impact. The conductivity of brine is important for the interpretation of the resistivity of a porous media saturated with a conductive fluid (brine) and a non conductive fluid (hydrocarbons, $CO_2$). During $CO_2$ injection in any state (gas, supercritical), a thermodynamic equilibrium will rapidly take place behind the front and a fraction of $CO_2$ will be dissolved in water, therefore changing slightly its resistivity. When measuring in-situ resistivity using logging

tools or permanent sensors [4] with the objective of determining saturation, the simplest approach to calculate the saturation Sw is to use the Archie's laws:

$$Sw = \left( \frac{a\Phi^{-m}}{R_t} \right)^{1/n} Rw^{1/n} \tag{7}$$

where $R_t$ is the measured resistivity, $\Phi$ is porosity, $R$w is the brine resistivity (inverse of conductivity) and a, m and n are parameters that can be measured in the laboratory. The exponents m and n take values around 2 and typically vary in a range [1.5 – 2.5]. The sensitivity to the brine resistivity is easily derived:

$$\frac{dSw}{Sw} = \frac{1}{n} \frac{dRw}{Rw} \tag{8}$$

Hence, a relative variation of 10% of the brine resistivity will generate a relative variation of saturation of 5% when taking n=2. If this effect is not taken into account, saturation will be underestimated by 5%.

For viscosity, the increase of viscosity during dissolution of $CO_2$ will impact the time scale of convection due to the slight density difference between the formation brine and brine containing dissolved $CO_2$ [5]. If we consider a porous layer of thickness $H$ and porosity $\Phi$ in which a gradient of dissolved $CO_2$ concentration exists, a key parameter for describing the stability of the system is the Darcy-Rayleigh number defined as:

$$Ra = \frac{g \, \Delta\rho \, K \, H}{\eta \, \Phi \, D} \tag{9}$$

where $g$ is gravity, $D$ is diffusivity, $K$ is permeability and $\Delta\rho$ is the density difference due to the dissolved $CO_2$. The dissolved $CO_2$ being at the top of the layer, a density-driven convection can occur. But this density difference will fade away by molecular diffusion, and the speed of convection will depend on viscosity. Furthermore, following Xu et al. [5] in their stability analysis, the minimum time needed to develop an instability (or start convection) is given by:

$$t_c \propto \frac{(\eta \, \Phi)^2 \, D}{g \, \Delta\rho \, K} \tag{10}$$

This time depends on the square of viscosity and therefore may increase with increasing viscosity. However, the diffusivity may also decreased as a function of $CO_2$ concentration and partially compensate the viscosity effect.

## 5. Conclusion

The effect of dissolved $CO_2$ on the resistivity and viscosity of aqueous NaCl solutions is small and can be modeled using a simple linear function involving the mole fraction. The experiments have been performed on three NaCl solutions covering the range of salinity usually encountered in potential $CO_2$ storage geological formations. At a constant temperature of 35 °C, we show that the variation of conductivity and viscosity are both proportional to the mole fraction of dissolved $CO_2$. The relative variation of viscosity is slightly larger than the relative variation of conductivity. We propose a simple model to take into account the effect of both dissolved $CO_2$ and temperature. For resistivity to saturation conversion using the Archie's laws, a systematic underestimation of saturation of about 5% may be present if the slight increase of conductivity is not taken into account. Concerning viscosity, the time scale for the onset of convection may be underestimated if the increase of viscosity is not taken into account.

## 6. References

1 S. Bando, F. Takemura, M. Nishio, E. Hihara and M. Akai, J. Chem. Eng. Data 49 (2004) 1328.

2 J.F. Dufrêche, M. Jardat, P. Turq and B. Bagchi, J. Phys. Chem. B 112 (2008) 10264.

3 J.J. Arps, Trans. A.I.M.E. 198 (1953) 327.

4 A. Forster, B. Norden, K. Zinck-Jørgensen, P. Frykman, J. Kulenkampff, E. Spangenberg, J. Erzinger, M. Zimmer, J. Kopp, G. Borm, C. Juhlin, C. Cosma and S. Hurter, Env. Geosc. 13-3 (2006) 145.

5 X. Xu, S. Chen and D. Zhang, Adv. Water Res. 29 (2006) 397.